First in-beam gamma-ray study of the level structure of neutron-rich S-39

Chapman, R.; Wang, Z. M.; Bouhelal, M.; Haas, F.; Liang, X.; Azaiez, F.; Behera, B. R.; Burns, M.; Caurier, E.; Corradi, L.; Curien, D.; Deacon, A. N.; Dombradi, Zs.; Farnea, E.; Fioretto, E.; Gadea, A.; Hodsdon, A.; Ibrahim, F.; Jungclaus, A.; Keyes, K.; Kumar, V.; Lunardi, S.; Marginean, N.; Montagnoli, G.; Napoli, D. R.; Nowacki, F.; Ollier, J.; O'Donnell, D.; Papenberg, A.; Pollarolo, G.; Salsac, M. -D.; Scarlassara, F.; Smith, J. F.; Spohr, Klaus; Stanoiu, M.; Stefanini, A. M.; Szilner, S.; Trotta, M.; Verney, D.

Published in:
Physical Review C

DOI:
10.1103/PhysRevC.94.024325

Published: 17/08/2016

Document Version
Peer reviewed version

First in-beam gamma-ray study of the level structure of neutron-rich ^{39}S

R. Chapman,[1,*] Z. M. Wang,[1] M. Bouhelal,[2] F. Haas,[3] X. Liang,[1] F. Azaiez,[4] B. R. Behera,[5] M. Burns,[1] E. Caurier,[3] L. Corradi,[5] D. Curien,[3] A. N. Deacon,[6] Zs. Dombrádi,[7] E. Farnea,[8] E. Fioretto,[5] A. Gadea,[5] A. Hodsdon,[1] F. Ibrahim,[4] A. Jungclaus,[9] K. Keyes,[1] V. Kumar,[1] S. Lunardi,[8] N. Mărginean,[5,10] G. Montagnoli,[8] D. R. Napoli,[5] F. Nowacki,[3] J. Ollier,[1,11] D. O'Donnell,[1] A. Papenberg,[1] G. Pollarolo,[12] M.-D. Salsac,[13] F. Scarlassara,[8] J. F. Smith,[1] K. M. Spohr,[1] M. Stanoiu,[10] A. M. Stefanini,[5] S. Szilner,[5,14] M. Trotta,[5] and D. Verney[4]

[1] *School of Engineering and Computing, University of the West of Scotland, Paisley, PA1 2BE, United Kingdom and the Scottish Universities Physics Alliance (SUPA)*
[2] *Laboratoire de Physique Appliquée et Théorique, Université Larbi Tébessa, Tébessa, Algérie*
[3] *IPHC, CNRS-IN2P3 and Université de Strasbourg, F-67037 Strasbourg Cedex 2, France*
[4] *IPN, CNRS-IN2P3 and Université Paris-Sud, F-91406 Orsay Cedex, France*
[5] *INFN, Laboratori Nazionali di Legnaro, I-35020 Legnaro, Padova, Italy*
[6] *Schuster Laboratory, University of Manchester, Manchester, M13 9PL, United Kingdom*
[7] *ATOMKI, P.O. Box 51, H-4001 Debrecen, Hungary*
[8] *Dipartimento di Fisica and INFN-Sezione di Padova, Università di Padova, I35131 Padova, Italy*
[9] *Instituto de Estructura de la Materia, CSIC, E-28006 Madrid, Spain*
[10] *Horia Hulubei National Institute of Physics and Nuclear Engineering, Strasse Atomistilor 407, P. O. BOX MG-6, Bucharest, Romania*
[11] *STFC Daresbury Laboratory, Warrington, WA4 4AD, United Kingdom*
[12] *Dipartimento di Fisica Teorica, Universitá di Torino, and INFN-Sezione di Torino, Via P. Giuria 1, I-10125 Torino, Italy*
[13] *CEA-Saclay, Service de Physique Nucléaire, 91191 Gif-sur-Yvette, France*
[14] *Ruder Bošković Institute, Zagreb, Croatia*

(Dated: July 28, 2016)

The neutron-rich ^{39}S nucleus has been studied using binary grazing reactions produced by the interaction of a 215-MeV beam of ^{36}S ions with a thin ^{208}Pb target. The magnetic spectrometer, PRISMA, and the γ-ray array, CLARA, were used in the measurements. Gamma-ray transitions of energy 339, 398, 466, 705, 1517, 1656, and 1724 keV were observed. Five of the observed transitions have been tentatively assigned to the decay of excited states with spins up to $(11/2^-)$. The results of a state-of-the-art shell-model calculation of the level scheme of ^{39}S using the SDPF-U effective interaction are also presented. The systematic behaviour of the excitation energy of the first $11/2^-$ states in the odd-A isotopes of sulphur and argon is discussed in relation to the excitation energy of the first excited 2^+ states of the adjacent even-A isotopes. The states of ^{39}S which have the components in their wave functions corresponding to three neutrons in the $1f_{7/2}$ orbital outside the $N = 20$ core have also been discussed within the context of 0 $\hbar\omega$ shell-model calculations presented here.

I. INTRODUCTION

The present paper is concerned with the nuclear structure of $^{39}_{16}S_{23}$ and forms the last of a series of studies of neutron-rich nuclei lying between the $N = 20$ and 28 shell closures which have been based on the same experiment carried out at the INFN Legnaro National Laboratory, Italy. Binary grazing reactions were used to populate the nuclei of interest. The previous published works from the experiment have involved studies of the neutron-rich isotopes ^{33}Si [1], ^{36}Si [2], ^{34}P [3], ^{35}P [3], ^{36}P [3], ^{37}P [3], ^{38}P [3], ^{37}S [4], ^{40}S [5], ^{41}S [6], and ^{38}Cl [7]. These studies are mainly concerned with the role of negative-parity intruder orbitals in the structure of neutron-rich nuclei on the periphery of the island of inversion, which is centred on ^{32}Mg, and on the description of such nuclei using state-of-the-art shell-model calculations [8]. Binary grazing and deep-inelastic reactions have been used extensively over the last few decades to study the structure of neutron-rich nuclei over a wide range of nuclear masses. The coupling of large solid-angle magnetic spectrometers to arrays of escape-suppressed Ge detectors in studies of this type (see e.g. Refs. [9–11]) has represented a very significant experimental advance in relation to earlier techniques which exploited large arrays of Ge detectors but no particle identification, see e.g. Broda *et al.* [12], Fornal *et al.* [13], and Lee *et al.* [14].

In an earlier publication [5], we discussed the evolving structure of the sulphur isotopes for neutron numbers, $22 \leq N \leq 28$. The large energy gap between the $1d_{3/2}$ and $2s_{1/2}$ proton shell-model states at $N = 20$ ^{36}S reinforces the effects of the neutron shell closure and this is reflected in a large 2^+ energy (3.29 MeV) and small $B(E2;0^+ \to 2^+)$ value (88.6 ± 7.0 e^2 fm^4) [15]. In the $N = 20$ odd-A isotones, ^{35}P and ^{37}Cl, the energy gap, $E(1/2^+_1)$ - $E(3/2^+_1)$ is approximately -2.5 MeV and 1.75 MeV, respectively [16]. With increasing neutron number, the energy spacing of the proton $1d_{3/2}$ and $2s_{1/2}$ orbitals decreases as the $1f_{7/2}$

*Electronic address: Robert.Chapman@uws.ac.uk

neutron orbit is filled; this is a consequence of the attractive monopole tensor force [17] between $1f_{7/2}$ ($j_>$) neutrons and protons in the $1d_{3/2}$ ($j_<$) orbit. For the isotopes of potassium, where the energy spacing has been measured using proton pickup reactions [18, 19], the total monopole shift between $1d_{3/2}$ and $2s_{1/2}$ proton binding is about 350 keV per $1f_{7/2}$ neutron [20]. The decreasing $1d_{3/2}$ - $2s_{1/2}$ proton energy spacing with increasing neutron number is the underlying reason for the increase in quadrupole deformation in the even-A sulphur isotopes [21, 22]; a pseudo-SU(3) symmetry develops [23] with increasing neutron number. In addition, as neutrons are added to the $1f_{7/2}$ shell, there is a tendency for the nucleus to adopt a quadrupole deformation in order to remove the degeneracy associated with the increasing occupancy of the $1f_{7/2}$ shell. This is the nuclear analogue of the Jahn-Teller effect [24, 25], which was first discussed in 1937 in relation to the stability of polyatomic molecules in degenerate electronic states [26].

From the simple perspective of the nuclear shell model, the ${}^{39}{}_{16}S$ ground state has 4 proton holes in the sd shell and 3 neutrons in the $1f_{7/2}$ orbital outside the $N = 20$ shell closure, with a J^π value of $7/2^-$. The three neutrons in the $1f_{7/2}$ orbit would be expected to play a dominant role in the low-lying excited states; they can couple to J^π values of $3/2^-$, $5/2^-$, $7/2^-$, $9/2^-$, $11/2^-$, and $15/2^-$; J^π values of $1/2^-$ and $13/2^-$ are forbidden by quantum-mechanical angular momentum coupling considerations. However, the shell-model calculations of Woods [27] show that neutron excitations into the $2p_{3/2}$ orbital play an important role in the structure of the close lying triplet of states with J^π values of $7/2^-$, $5/2^-$, and $3/2^-$ (ground state). The configuration $\pi(2s_{1/2}1d_{3/2})^2 \otimes \nu(1f_{7/2})^3$ contributes 65 %, 44 %, and 42 % to the total wave function, respectively, while the neutron occupancies of the $2p_{3/2}$ orbital are 0.32, 0.50, and 0.77, respectively.

There have been few experimental studies of the neutron-rich ${}^{39}{}_{16}S$ nucleus and no conclusive in-beam γ-ray studies. Drumm *et al.* [28], using the ${}^{40}Ar({}^{13}C,{}^{14}O){}^{39}S$ transfer reaction, observed a level with a large energy uncertainty at 1469±25 keV. A further study of ${}^{39}S$ using β decay was performed by Winger *et al.* [29]. Gamma rays of energies 339.8, 398.2, 1126.2, and 1524.6 keV were observed; however there was not enough supporting information to place these four γ-ray transitions within a ${}^{39}S$ level scheme. In a β-delayed neutron emission study by Winger *et al.* [30], 339.9- and 398.6-keV γ rays were observed to be in coincidence with 465.5-keV γ rays, but not with each other. As a by-product of an investigation of the level structure of ${}^{45,46}Ar$ through in-beam γ-ray spectroscopy using the fragmentation of a 60 AMeV ${}^{48}Ca$ beam, Dombrádi et al. [31] identified a γ-ray transition of energy 904(7) keV, which was attributed to ${}^{39}S$. Thus, although the 339.9-, 398.6-, 465.5-, 904-, 1126.2-, and 1524.6-keV γ rays have been assigned to the decay of excited states of ${}^{39}S$, to date none has been placed within a level scheme.

Binary grazing reactions with stable neutron-rich beams and heavy targets can be used to populate yrast and near-yrast states of moderately neutron-rich projectile-like species [5, 13, 32–34] and, in general, experiments using such reactions, although unable to reach the most neutron-rich nuclear species currently accessible to experiment, provide more detailed spectroscopy than is currently possible using intermediate-energy Coulomb excitation, where the states that are populated are, in general, those that are connected directly to the ground state by E2 transitions [35]. Fusion-evaporation reactions with stable beams are unable to populate neutron-rich nuclei such as ${}^{39}S$. Here, the yrast decay sequence of ${}^{39}S$, populated in binary grazing reactions, has been studied. We have exploited the combination of a large acceptance magnetic spectrometer, PRISMA [36, 37], and a high granularity and high efficiency γ-ray detection array, CLARA [38], which allows good reaction channel selection and precise Doppler correction of γ-ray energy spectra.

II. EXPERIMENT

Yrast and near-yrast states of the $N = 23$ nucleus ${}^{39}S$ were populated using binary grazing reactions produced in the interaction of a 215 MeV beam of ${}^{36}S^{9+}$ ions, delivered by the Tandem-ALPI accelerator complex at the INFN Legnaro National Laboratory, Italy, with a thin ${}^{208}Pb$ target. The target, isotopically enriched to 99.7% in ${}^{208}Pb$, was of thickness 300 $\mu g\ cm^{-2}$ on a 20 $\mu g\ cm^{-2}$ carbon backing. Projectile-like fragments produced during the reaction were analyzed with PRISMA [36, 37], a large acceptance-angle magnetic spectrometer placed at 56° to the beam axis, and covering a range of angles including the grazing angle of the reaction (58°). Measurements taken with the PRISMA magnetic spectrometer enable a determination of the atomic number Z, the mass number A, the ionic charge state, and the absolute velocity vector of each ion that reaches the detector system at the focal plane. PRISMA has a solid angle of 80 *msr*, a momentum acceptance of ±10%, and a mass resolution of 1/300 via time of flight measurements. Gamma rays from the de-excitation of projectile- and target-like binary reaction products were detected using CLARA [38], an array of 25 escape-suppressed Ge clover detectors (22 Ge clover detectors were used during the present work). The CLARA array has a photopeak efficiency of about 3%, a peak-to-total ratio of 0.45 for ${}^{60}Co$ 1332-keV γ rays, and covers an azimuthal angular range of $\theta = 98°$ to 180° with respect to the entrance aperture of the PRISMA magnetic spectrometer. Following Doppler-shift energy correction of γ rays from projectile-like species, the FWHM of γ-ray photopeaks is approximately 0.7% in energy. A relative photopeak efficiency calibration for the CLARA array was carried out using radioactive sources of ${}^{152}Eu$, ${}^{133}Ba$, and ${}^{56}Co$. Gamma rays were detected in time coincidence with projectile-like fragments identified at the focal plane of the PRISMA spectrometer, thereby providing an unambiguous association of γ rays with each projectile-like binary fragment of a particular A and Z. The data acquisition trigger is provided by timing signals from the large area multi-wire parallel plate avalanche counter (MWPPAC) at the focal plane of PRISMA. Doppler correction of γ-ray energies was performed on an event-by-event basis. More details of the experimental equipment used here have been given in earlier publications e.g. [5]. Experimental data were accumulated during a six day run with an average beam current of 7 pnA.

III. RESULTS AND DISCUSSION

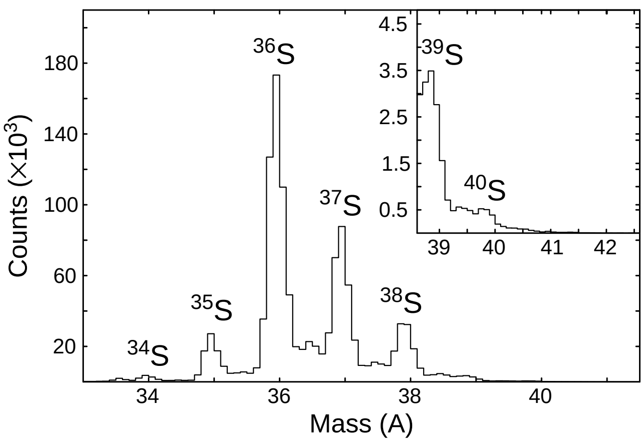

FIG. 1: Mass spectrum for sulphur ($Z = 16$) isotopes (measured in coincidence with γ rays) populated in the present work. See text for details.

In the present experiment, a wide range of nuclear species, from Mg ($Z = 12$) to Ca ($Z = 20$), was identified at the focal plane of PRISMA. Here, we focus on a discussion of ^{39}S. ^{39}S was weakly populated in a three-neutron transfer reaction with 16200±130 γ-particle coincident events recorded. Figure 1 shows the γ-A matrix (projected onto the mass axis) which resulted from the correlation of γ rays and detected S ions. Electronic timing problems during the experiment resulted in tails on the mass peaks (see Fig. 1); any resulting contamination of the γ-ray spectra can be readily identified through the generation of γ-ray spectra corresponding to each of the sulphur isotopes and through the use of mass gates of different widths.

Figure 2 presents the Doppler-corrected singles γ-ray energy spectrum measured in coincidence with ^{39}S ions identified at the focal plane of PRISMA. The γ-ray spectrum has photopeaks at energies of 339(1), 398(1), 466(1), 705(1), 1517(1), 1656(1), and 1724(1) keV. As noted earlier, the 339-, 398-, and 466-keV γ-ray transitions were previously identified by Winger *et al.* [29, 30]; however, the 1126.2- and 1524.6-keV γ-ray transitions observed by Winger *et al.* and that observed by Dombrádi *et al.* [31] at an energy of 904 keV, were not observed here. The measured ^{39}S γ-ray energies and relative intensities are presented in Table I.

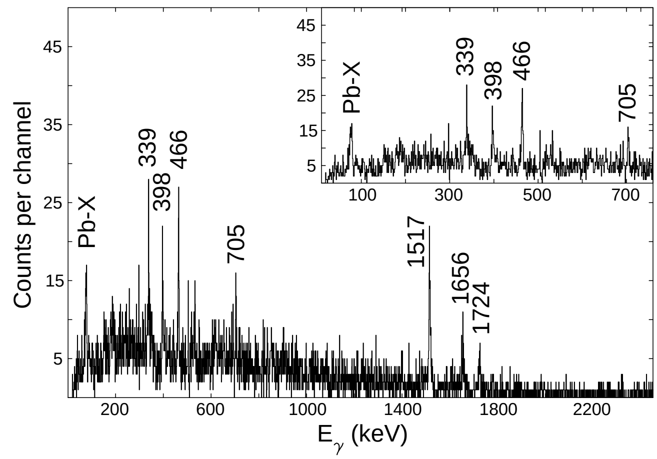

FIG. 2: Gamma-ray singles energy spectrum observed in coincidence with ^{39}S ions detected at the focal plane of PRISMA.

The γ-ray spectrum corresponding to the decay of the associated target-like fragments is presented in Fig. 3; Doppler correction of this γ-ray spectrum was performed assuming two-body kinematics. The observed γ-ray peaks correspond to the de-excitation of known states of ^{205}Pb. In particular, the γ-ray peaks at energies of 323, 684, and 703 keV correspond to the previously observed yrast transitions [39] from $19/2^+$ to $17/2^+$, $17/2^+$ to $13/2^+$, and $7/2^-$ to $5/2^-$, respectively. On the other hand, the strong photopeak at 803 keV does not correspond to a previously observed transition of ^{205}Pb; the relative photopeak intensity would suggest that the peak corresponds to the deexcitation of an yrast state. The ${2_1}^+ \rightarrow 0^+$ transition in ^{206}Pb has an energy of 803.1 keV; it is the strongest photopeak in the γ-ray spectrum of the associated target-like fragments observed in coincidence with ^{38}S ions detected at the focal plane in the same experiment [40]. Thus, contamination of the ^{39}S mass peak by the much more intense ^{38}S peak (see Fig. 1) may account for the presence of the 803-keV peak in the spectrum of Fig. 3. On the other hand, the strongest transition observed in the ^{38}S γ-ray spectrum at 1292 keV (${2_1}^+ \rightarrow 0^+$) [40] is not present in the spectrum of Fig. 2. There is no convincing evidence in the spectrum of Fig. 3 for the population of the 899.2-keV first 2^+ state of ^{204}Pb [41]; this indicates that neutron evaporation of the excited target-like fragment is not a significant process in this particular case. Photopeaks marked with "Pb-X" in Fig. 2 and in Fig. 3 are lead x rays from the target.

The statistics in the experiment were not adequate in order to perform a γ-γ coincidence analysis, necessary

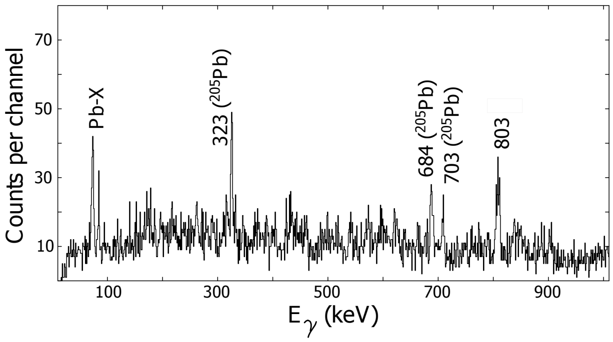

FIG. 3: One dimensional Doppler-corrected γ-ray energy spectrum from target-like fragments observed in association with ^{39}S ions detected at the focal plane of the PRISMA spectrometer. All but one of the observed photopeaks can be associated with known γ-ray transitions in ^{205}Pb. See text for details.

TABLE I: Measured γ-ray transition energies and relative intensities for ^{39}S. Previously unobserved γ-ray transitions are indicated by the symbol *.

E_γ(keV)	I_γ/I_{1517} (%)
339(1)	17.3(2.4)
398(1)	18.1(2.7)
466(1)	24.1(3.2)
705(1)*	12.6(2.7)
1517(1)*	100.0(6.5)
1656(1)*	34.3(4.9)
1724(1)*	27.2(4.1)

for the construction of a robust level scheme. Rather, the proposed ^{39}S level scheme is based on several considerations, namely comparison with the published level schemes of the $N = 23$ isotones, ^{37}Si and, in particular, ^{41}Ar, and with the results of shell-model calculations for ^{39}S, also presented here. Further, as noted earlier, binary grazing reactions of the type discussed here preferentially populate yrast and near-yrast states of the final nuclei. The level scheme must also be consistent with the measured relative transition intensities (Table I). Finally, as noted above, in the work of Winger *et al.* [30] the 339.9- and 398.6-keV γ rays were observed to be in coincidence with 465.5-keV γ rays, but not with each other.

Figure 4 shows partial level schemes for the $N = 23$ isotones, ^{37}Si, ^{39}S, and ^{41}Ar. The level scheme for ^{37}Si is based on the work of Steiger *et al.* [42] and of Stroberg *et al.* [43]. For ^{41}Ar, the level scheme of Szilner *et al.* [44] is presented; in this work, the PRISMA/CLARA detector systems were used, as in the present study, and states of ^{41}Ar were populated in a binary grazing reaction initiated by an ^{40}Ar beam on a ^{208}Pb target. Consequently, there are expected to be some similarities with the yrast and near-yrast excited states of ^{39}S based on the present work; however, since the states of ^{41}Ar were populated in a one-neutron transfer reaction, single-neutron states are also expected to be strongly populated in this case, and this is what is observed experimentally [44]. It is proposed that the strongest observed γ-ray photopeak at 1517-keV in the spectrum of Fig. 2 corresponds to a transition from a $J^\pi = 11/2^-$ state at 1517 keV to the ground state. The energy of the state is two standard deviations from that measured by Drumm *et al.* [28] at 1469±25 keV. The corresponding state in ^{41}Ar lies at an excitation energy of 1630 keV and is also relatively strongly populated. The first $J^\pi = 9/2^-$ state, predicted in the shell-model calculations presented here to lie at an excitation energy of 1803 keV, is also expected to be strongly populated and, on this basis and by comparison with the ^{41}Ar level scheme, the 1656-keV transition is very tentatively assigned to the decay of a 1656-keV $J^\pi = 9/2^-$ state to the ground state. The 1656-keV transition is, in this proposed placement, favoured over the 1724-keV transition because of its higher intensity; confirmation of the placement through γ-γ coincidence measurements is necessary. The 466-, 389-, and 339-keV transitions have been assigned to low-lying states of ^{39}S through a comparison with the $3/2^-_1$, $5/2^-_1$, $7/2^-_1$, and $3/2^+_1$ levels of ^{37}Si and ^{41}Ar. It is again emphasised that the ^{39}S level scheme presented here should be regarded as tentative; good statistics γ-γ coincidence data are required to confirm the proposed placement of γ rays. Thus, of the seven γ-ray transitions listed in Table I, five have been tentatively placed in the ^{39}S level scheme and two transitions, those at 705 keV and 1724 keV, have not been included because of the lack of supporting evidence. In the experiment of Szilner *et al.*, to which reference has been made above, γ-ray photopeaks of energy 339(1), 399(1), 467(1), 535(1), 1518(1), 1654(2), and 1727(4) keV were observed in the -2p + 1n channel, ^{208}Pb(^{40}Ar,^{39}S) [45]. The 535-keV transition was not observed in the present work and the 705-keV transition was not observed in the work of Szilner *et al.* [45].

A large scale 0 $\hbar\omega$ shell-model calculation was performed to understand the structure of ^{39}S from a theoretical aspect using the Nathan code [8, 46] with the latest SDPF-U effective interaction [47]. Protons are restricted to the sd shell and neutrons are confined to the full pf shell-model space outside an inert ^{28}O core. The results of the shell-model calculation are presented in Fig. 4.

The ground-state configuration of the even-Z $N = 23$ isotones, in a simple shell-model picture, is described in terms of the coupling of three extra-core $1f_{7/2}$ neutrons to an inert proton core. In some cases, the lowest state of such a $(j)^3$ configuration has a total angular momentum quantum number of $J = j - 1$, rather than $J = j$. This is a consequence of the residual interaction between the three like nucleons in the same orbit and was first discussed by Talmi in 1962 [48]. In ^{37}Si$_{23}$, shell-model calculations performed here, and based on the SDPF-U

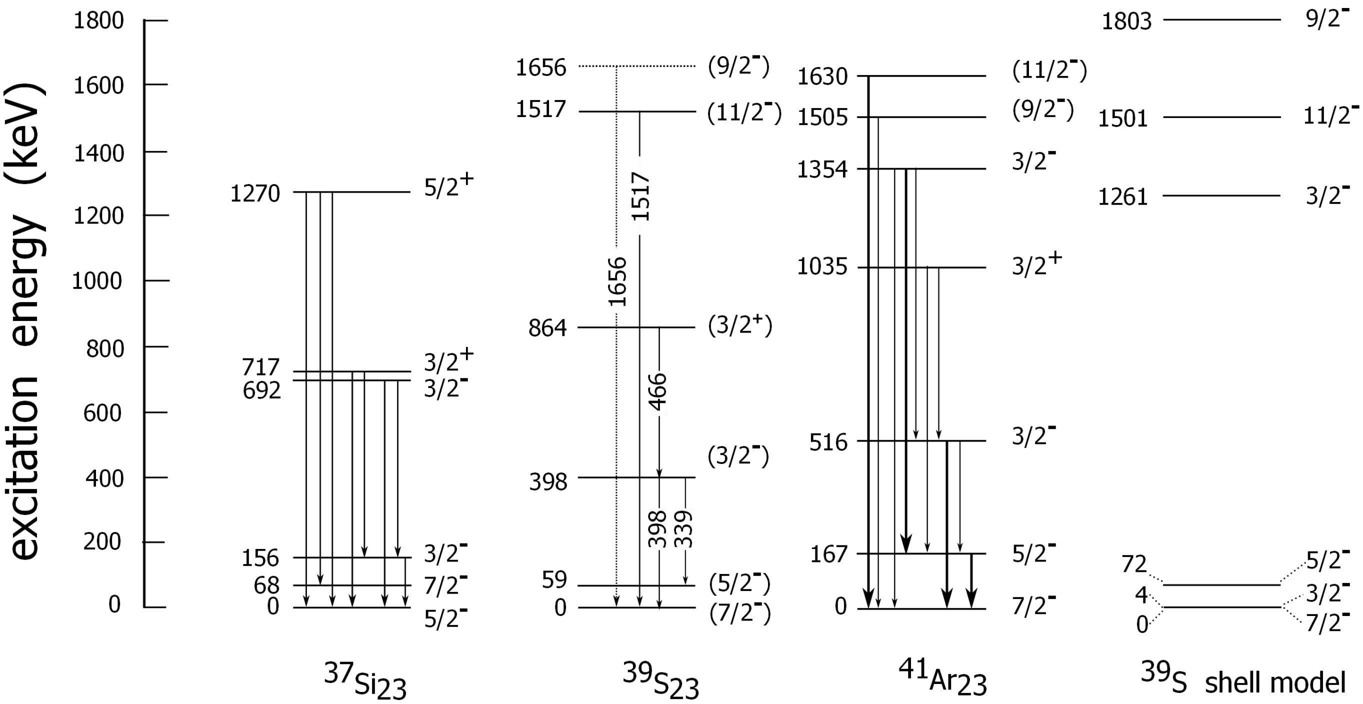

FIG. 4: Partial level schemes of the $N = 23$ isotones, ^{37}Si and ^{41}Ar together with the proposed level scheme of ^{39}S. The results of shell-model calculations based on the SDPF-U effective interaction are also presented. See text for details.

interaction, give a ground-state J^π value of $5/2^-$, a first excited state at an excitation energy of 170 keV with J^π value of $7/2^-$, and a second excited state at 237 keV with a J^π value of $3/2^-$. The experimental level scheme (Fig. 4) is consistent with this. However, there has been no definitive determination of the ground-state J^π value; the adopted value of $7/2^-$ [49], which is in disagreement with the more recent work of Steiger *et al.* [42] and of Stroberg *et al.* [43], is based on systematics. For the ground state, the largest component ($\sim 38\%$) of the wave function corresponds to three $1f_{7/2}$ neutrons coupled to an inert $(1d_{5/2})^6$ proton core; 70 % of the wave function corresponds to neutrons coupled to spin $5/2^-$ and protons to 0^+. In the case of ^{41}Ar$_{23}$, the shell-model predicts close-lying $J^\pi = 5/2^-$ (ground) and $7/2^-$ (36-keV first excited) states, with the $J^\pi = 3/2^-$ state at 783 keV. The experimental ground-state J^π value of $7/2^-$ is based on the results of (d,p) single neutron transfer studies with a polarised deuteron beam [50, 51]; the largest component ($\sim$ 65%) of the wave function corresponds to three $1f_{7/2}$ neutrons coupled to protons with the configuration $(1d_{5/2})^6(2s_{1/2})^2(1d_{3/2})^2$. Shell-model calculations for ^{39}S give a ground-state J^π value of $7/2^-$, with close-lying $3/2^-$ (4 keV) and $5/2^-$ (72 keV) states. The adopted ground-state J^π value ($7/2^-$) [52] is based on systematics. In the present work, the assumption is made that the ground-state J^π value is $7/2^-$ but, as is also the case for the ^{37}Si ground-state, no definitive model-independent assignment has so far been made. Within the context of shell-model calculations, the ordering of the low-lying states in the $N = 23$ isotones is sensitive to details of the interaction. The ground state of ^{39}S has, as the three largest components of the wave function, the neutron configuration $(1d_{5/2})^6(2s_{1/2})^2(1d_{3/2})^4(1f_{7/2})^3$ with the proton configurations $(1d_{5/2})^6(2s_{1/2})^2(1d_{3/2})^0$ (17%), $(1d_{5/2})^6(2s_{1/2})^0(1d_{3/2})^2$ (20%), and $(1d_{5/2})^6(2s_{1/2})^1(1d_{3/2})^1$ (21%). The nearby shell-model excited states at 4 keV ($J^\pi = 3/2^-$) and at 72 keV ($J^\pi = 5/2^-$) have the same above three configurations in their wave functions with corresponding contributions of 10-, 14-, and 17 % and of 22-, 19-, and 13 %, respectively. Contrary to the expectations of the simple shell model, these states cannot be described in terms of three $1f_{7/2}$ neutrons coupled to an inert proton core.

The second $3/2^-$ shell-model state in ^{39}S at 1261 keV has the dominant component (42%) in its wave function corresponding to the promotion of a neutron from the $1f_{7/2}$ to the $2p_{3/2}$ shell, namely $\nu(1d_{3/2})^4(1f_{7/2})^2(2p_{3/2})^1 \otimes \pi(1d_{5/2})^6(2s_{1/2})^2$; 69% of the wave function corresponds to neutrons with $J^\pi = 3/2^-$ coupled to protons with $J^\pi = 0^+$. Consequently, the state is not expected to be strongly populated in the present work. The second $3/2^-$ state of ^{37}Si at an experimental excitation energy of 692 keV has a very similar shell-model structure; the state was populated in a one-neutron knockout reaction [43] with a spectroscopic factor consistent with the results of a shell-model calculation, which used the SDPF-U effective interaction. The largest component of the wave function (33%) is $\pi(1d_{5/2})^6 \otimes \nu(1d_{3/2})^4(1f_{7/2})^2(2p_{3/2})^1$. In the work of Szilner *et al.*, the most strongly populated state of ^{41}Ar is that at 1354 keV with a J^π value of $3/2^-$; this state has a pronounced single-particle character. In the ^{40}Ar(d,p)^{41}Ar single-neutron transfer study of Sen *et al.* [50], the measured transfer strength to the state is $(2J+1)S = 1.7 \pm 0.3$, which is consistent, within the normal uncertainties associated with a Distorted Wave Born Analysis (DWBA) of single nucleon transfer cross section measurements, with the shell-model wave function, $\pi(1d_{5/2})^6(2s_{1/2})^2(1d_{3/2})^2 \otimes \nu(1d_{3/2})^4(1f_{7/2})^2(2p_{3/2})^1$ (53%). The intruder $3/2_1^+$ state has been observed in all three isotones (Fig. 4). Population of the state in ^{37}Si at 717 keV by the removal of a $1d_{3/2}$ neutron with a spectroscopic factor of $C^2S = 1.5$ [43] and the weak population ($C^2S = 0.06$) of the equivalent state at 1035 keV in the ^{40}Ar(d,p)^{41}A reaction [52] are consistent with the main component of the wave function corresponding to $\nu(1d_{3/2})^3(1f_{7/2})^4$. Such positive parity states lie outside the 0 $\hbar\omega$ configuration space of the present shell-model calculations.

In the present shell-model calculations for ^{39}S, the energy gap of about 1200 keV between the low-lying triplet of states and the second $J^\pi = 3/2^-$ state would suggest that higher-lying states have significant core-coupling components in their wave functions. For the first $11/2^-$ shell-model state, for which the proposed experimental counterpart is at 1517 keV, the component of the wave function corresponding to protons coupled to a J^π value of 2^+ and neutrons coupled to $7/2^-$ corresponds to 33% of the total wave function. The largest component of the wave function (45%) corresponds to neutrons coupled to a J^π value of $11/2^-$ and protons to $J^\pi = 0^+$. Seventeen percent of the total wave function corresponds to three neutrons in the $1f_{7/2}$ orbital coupled to an inert proton core, $(1d_{5/2})^6(2s_{1/2})^2$, whereas 22% corresponds to the three $1f_{7/2}$ neutrons coupled to the proton configuration $(1d_{5/2})^6(2s_{1/2})^1(1d_{3/2})^1$. In a particle-core coupling description, states of ^{39}S can be considered as a ^{38}S core coupled to the unpaired neutron in the $1f_{7/2}$ orbital. Such a particle-core coupling description has been found to have some validity in earlier work in this region e.g. see refs. [4, 53, 54]. The excitation energy of the first 2^+ state of ^{38}S is 1292 keV [55] and this suggests that a particle-core coupling description is appropriate for the 1517-keV $J^\pi = (11/2^-)$ state of ^{39}S. Figure 5 presents, for the isotopes of sulphur and argon, with neutron numbers in the range from 14 to 28, the excitation energies of the first 2^+ states in the even-A isotopes and the excitation energy differences of the first $11/2^-$ and first $7/2^-$ states of the odd-A isotopes. The corresponding data for the isotopes of Si have not been presented, since information in relation to the odd-A isotopes is rather sparse. The data presented in the figure were taken from Nuclear Data Sheet references [49, 52, 55–72]. For the isotopes of sulphur and argon, the figure shows a good correlation between the behaviour of the excitation energy of the first 2^+ states of the even-A isotopes and the excitation energy differences of the first $11/2^-$ and first $7/2^-$ states of the odd-A isotopes with neutron number. The simple systematic behaviour presented in Fig. 5 suggests the applicability of a particle-core coupling model involving a $1f_{7/2}$ neutron coupled to the first 2^+ state of the even-even core. In particular, the effect of the neutron shell closures is very pronounced for both the even-A and odd-A isotopes and the decrease in excitation energies, $E(2_1^+)$ and $E(11/2_1^-)$ - $E(7/2_1^-)$, with increasing neutron number, together with the known behaviour of the $B(E2;0_{g.s.}^+ \rightarrow 2_1^+)$ values for the even-A sulphur and argon isotopes [15], reflect the increase in quadrupole collectivity with increasing neutron number. Experimental determination of the $B(E2;11/2_1^- \rightarrow 7/2_1^-)$ values would give a more definitive indication concerning the evolution of collectivity in the odd-A isotopes.

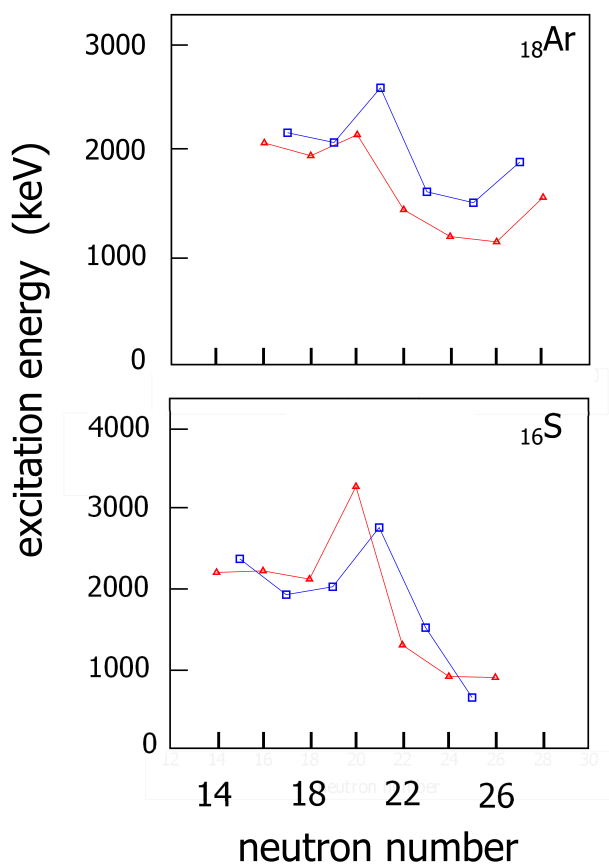

FIG. 5: Excitation energies of the first 2^+ states of the even-A isotopes of sulphur and argon for neutron numbers in the range from 14 to 28 (red triangles connected by red lines). Also shown are the excitation energy differences between the first $11/2^-$ and first $7/2^-$ states of the odd-A isotopes (blue squares connected by blue lines). See text for details.

In a simple shell-model picture, there are expected to be six states of ^{39}S which correspond to the various allowed couplings of three $1f_{7/2}$ neutrons which lie

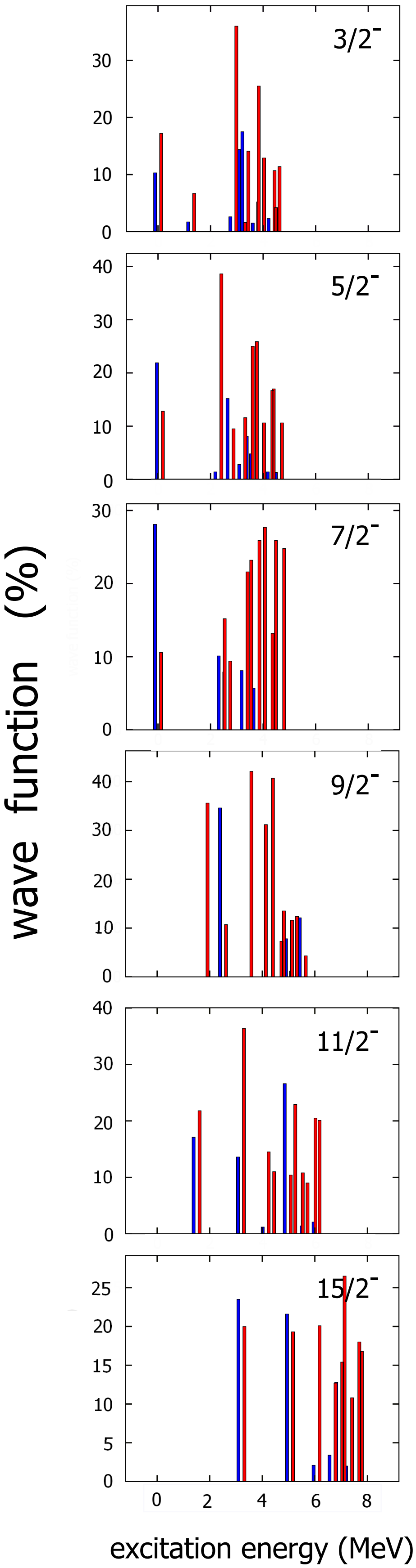

FIG. 6: Shell-model wave-function components corresponding to states of ^{39}S for which three neutrons in the 1f$_{7/2}$ orbital outside a closed $N = 20$ core are coupled to an inert $Z = 16$ proton core (blue). The red histograms correspond to the coupling of the three f$_{7/2}$ neutrons to protons with a (s$_{1/2}$)^1(d$_{3/2}$)^1 configuration. See text for details.

outside the $N = 20$ ^{36}S ground state core. Shell-model calculations performed here show that the ν(f$_{7/2}$)^3 strength is not concentrated in a single state for each of the possible J^π values, but rather the strength is distributed over many states encompassing a wide range of excitation energies. As noted earlier, the three neutrons in the 1f$_{7/2}$ orbital are forbidden, by angular momentum coupling considerations, to couple to total angular momentum values of $J^\pi = 1/2^-$ and $13/2^-$. Figure 6 shows the results of a shell-model calculation of the distribution of ν(f$_{7/2}$)^3 strength for states with J^π values of $3/2^-$, $5/2^-$, $7/2^-$, $9/2^-$, $11/2^-$, and $15/2^-$. The shell-model calculation used the SDPF-U effective interaction and the first ten states of each J^π value were included. The histogram in blue colour corresponds to the configuration $\pi(1d_{5/2})^6(2s_{1/2})^2 \otimes \nu(1d_{5/2})^6(2s_{1/2})^2(1d_{3/2})^4(1f_{7/2})^3$ in which the proton core is undisturbed, whereas the histogram in red corresponds to the configuration $\pi(1d_{5/2})^6(2s_{1/2})^1(1d_{3/2})^1 \otimes \nu(1d_{5/2})^6(2s_{1/2})^2(1d_{3/2})^4(1f_{7/2})^3$. The latter proton configuration is included in the figure since it plays an important role in the wave function of states for which there are three neutrons in the 1f$_{7/2}$ shell. It can be seen that there is a considerable distribution in energy of (f$_{7/2}$)^3 strength and that, as expected, the centroid of the strength increases with increasing J^π value. As mentioned earlier in relation to the three lowest-lying shell-model states, the simple shell-model picture of (f$_{7/2}$)^3 neutron strength carried by a multiplet of six states is evidently much too simplistic. The mixing of configurations in the wave functions of states of ^{39}S is probably a consequence of several nuclear effects. The development of a pseudo-SU(3) symmetry and the consequences of the Jahn-Teller effect with increasing occupancy of the neutron 1f$_{7/2}$ shell were briefly discussed earlier. The tendency for the nucleus to become deformed with increasing neutron number in the isotopes of sulphur will result in mixing of states and the consequent increased complexity of nuclear wave functions. In addition, core-coupling of the type discussed above will also conspire to render the simple shell-model picture of low-lying state of ^{39}S states invalid.

IV. CONCLUSIONS

Binary grazing reactions have been used to populate states of ^{39}S and a tentative level scheme has been constructed for the first time based on comparison with the level structure of the $N = 23$ isotones ^{37}Si and ^{41}Ar and with the results of $0\hbar\omega$ shell-model calculations. The systematic behaviour of the excitation energy difference E($11/2_1{}^-$) - E($7/2_1{}^-$) in the odd-A isotopes of sulphur and argon is discussed in relation to the excitation energy of the first excited 2^+ states of the adjacent even-A isotopes. The states of ^{39}S which have the components in their wave functions corresponding to three neutrons in the $1f_{7/2}$ orbital outside the $N = 20$ ^{36}S core have also been discussed within the context of 0 $\hbar\omega$ shell-model calculations presented here.

Acknowledgments

This work was supported in part by the EPSRC (UK) and by the European Union under contract number RII3-CT-2004-506065. Five of us (D.O., M.B., A.H., K.K., and A.P.) acknowledge financial support from the EPSRC. Z.M.W acknowledges support from ORSAS and from the University of the West of Scotland. A.N.D. acknowledges support from the STFC. A.J. acknowledges financial support from the Spanish Ministerio de Ciencia e Innovación under contracts FPA2007-66069 and FPA2009-13377-C02-02. Zs.D. acknowledges the financial support from OTKA Project No. K100835. The contribution of the accelerator and target-fabrication staff at the INFN Legnaro National Laboratory is gratefully acknowledged.

---

[1] Z. M. Wang, R. Chapman, X. Liang, F. Haas, M. Bouhelal, F. Azaiez, B. R. Behera, M. Burns, E. Caurier, L. Corradi, et al., Phys. Rev. C **81**, 064301 (2010).

[2] X. Liang, F. Azaiez, R. Chapman, F. Haas, D. Bazzacco, S. Beghini, B. R. Behera, L. Berti, M. Burns, E. Caurier, et al., Phys. Rev. C **74**, 014311 (2006).

[3] R. Chapman, A. Hodsdon, M. Bouhelal, F. Haas, X. Liang, F. Azaiez, Z. Wang, B. R. Behera, M. Burns, E. Caurier, et al., Phys. Rev. C. **92**, 044308 (2015).

[4] R. Chapman, Z. M. Wang, M. Bouhelal, F. Haas, X. Liang, F. Azaiez, B. R. Behera, M. Burns, E. Caurier, L. Corradi, et al., Phys. Rev. C **93**, 044318 (2016).

[5] Z. M. Wang, R. Chapman, X. Liang, F. Haas, F. Azaiez, B. R. Behera, M. Burns, E. Caurier, L. Corradi, D. Curien, et al., Phys. Rev. C **81**, 054305 (2010).

[6] Z. M. Wang, R. Chapman, X. Liang, F. Haas, M. Bouhelal, F. Azaiez, B. R. Behera, M. Burns, E. Caurier, L. Corradi, et al., Phys. Rev. C **83**, 024 (2011).

[7] D. O'Donnell, R. Chapman, X. Liang, F. Azaiez, F. Haas, S. Beghini, B. R. Behera, M. Burns, E. Caurier, L. Corradi, et al., Phys. Rev. C **81**, 024318 (2010).

[8] E. Caurier, G. Martínez-Pinedo, F. Nowacki, A. Poves, and A. P. Zuker, Rev. Mod. Phys. **77**, 427 (2005).

[9] D. Montanari, S. Leoni, D. Mengoni, J. J. Valiente-Dobon, G. Benzoni, N. Blasi, G. Bocchi, P. F. Bortignon, S. Bottoni, A. Bracco, et al., Phys. Rev. C **85**, 044301 (2012).

[10] S. Bhattacharyya, M. Rejmund, A. Navin, E. Caurier, F. Nowacki, A. Poves, R. Chapman, D. O'Donnell, M. Gelin, A. Hodsdon, et al., Phys. Rev. Lett. **101**, 032501 (2008).

[11] C. Louchart, A. Obertelli, A. Görgen, W. Korten, D. Bazzacco, B. Birkenbach, B. Bruyneel, E. Clément, P. J. Coleman-Smith, L. Corradi, et al., Phys. Rev. C **87**, 054302 (2013).

[12] R. Broda, M. Quader, P. Daly, R. Janssens, T. Khoo, W. Ma, and M. Drigert, Physics Letters B **251**, 245 (1990).

[13] B. Fornal, R. H. Mayer, I. G. Bearden, P. Benet, R. Broda, P. J. Daly, Z. W. Grabowski, I. Ahmad, M. P. Carpenter, P. B. Fernandez, et al., Phys. Rev. **C49**, 2413 (1994).

[14] I. Y. Lee, S. Asztalos, M.-A. Deleplanque, B. Cederwall, R. M. Diamond, P. Fallon, A. O. Macchiavelli, L. Phair, F. S. Stephens, G. J. Wozniak, et al., Phys. Rev. C **56**, 753 (1997).

[15] B. Pritychenko, M. Birch, B. Singh, and M. Horoi, Atomic Data and Nuclear Data Tables **107**, 1 (2016).

[16] A. Gade, B. A. Brown, D. Bazin, C. M. Campbell, J. A. Church, D. C. Dinca, J. Enders, T. Glasmacher, M. Horoi, Z. Hu, et al., Phys. Rev. C **74**, 034322 (2006).

[17] T. Otsuka, T. Suzuki, R. Fujimoto, H. Grawe, and Y. Akaishi, Phys. Rev. Lett. **95**, 232502 (2005).

[18] P. Doll, G. J. Wagner, K. T. Knopfle, and G. Mairle, Nucl. Phys. **A263**, 210 (1976).

[19] S. M. Banks, B. M. Spicer, G. G. Shute, V. C. Officer, G. J. Wagner, W. E. Dollhopf, Li Qingli, C. W. Glover, D. W. Devins, and D. L. Friesel, Nucl. Phys. **A437**, 381 (1985).

[20] O. Sorlin and M. G. Porquet, Prog. Part. Nucl. Phys. **61**, 602 (2008).

[21] H. Scheit, T. Glasmacher, B. A. Brown, J. A. Brown, P. D. Cottle, P. G. Hansen, R. Harkewicz, M. Hellstrom, R. W. Ibbotson, J. K. Jewell, et al., Phys. Rev. Lett. **77**, 3967 (1996).

[22] T. Glasmacher, B. A. Brown, M. J. Chromik, P. D. Cottle, M. Fauerbach, R. W. Ibbotson, K. W. Kemper, D. J. Morrissey, H. Scheit, D. W. Sklenicka, et al., Phys. Lett. B **395**, 163 (1997).

[23] J. Retamosa, E. Caurier, F. Nowacki, and A. Poves, Phys. Rev. C **55**, 1266 (1997).

[24] P. G. Reinhard and E. W. Otten, Nucl. Phys. **A420**, 173 (1984).

[25] W. Nazarewicz, Nucl. Phys. **A574**, 27c (1994).

[26] H. A. Jahn and E. Teller, Proc. R. Soc. London **A161**, 220 (1937).

[27] C. L. Woods, Nucl.Phys. **A451**, 413 (1986).

[28] P. V. Drumm, L. K. Fifield, R. A. Bark, M. A. C. Hotchkis, and C. L. Woods, Nucl.Phys. **A496**, 530 (1989).

[29] J. A. Winger, H. H. Yousif, W. C. Ma, V. Ravikumar, W. Lui, S. K. Phillips, R. B. Piercey, P. F. Mantica, B. Pritychenko, R. M. Ronningen, et al., AIP Conference Proceedings **455**, 606 (1998).

[30] J. A. Winger, P. F. Mantica, R. M. Ronningen, and M. A. Caprio, Phys. Rev. **C64**, 064318 (2001).

[31] Z. Dombradi, D. Sohler, O. Sorlin, F. Azaiez, F. Nowacki, M. Stanoiu, Y. E. Penionzhkevich, J. Timar, F. Amorini, D. Baiborodin, et al., Nucl.Phys. **A727**, 195 (2003).

[32] M. Guidry, S. Juutinen, X. Liu, C. Bingham, A. Larabee, L. Riedinger, C. Baktash, I. Lee, M. Halbert, D. Cline, et al., Physics Letters B **163**, 79 (1985).

[33] H. Takai, C. N. Knott, D. F. Winchell, J. X. Saladin, M. S. Kaplan, L. de Faro, R. Aryaeinejad, R. A. Blue,

R. M. Ronningen, and D. J. Morrissey, Phys. Rev. C **38**, 1247 (1988).
[34] X. Liang, R. Chapman, F. Haas, K. M. Spohr, P. Bednarczyk, S. M. Campbell, P. J. Dagnall, M. Davison, G. de Angelis, G. Duchene, et al., Phys. Rev. **C66**, 014302 (2002).
[35] A. Gade and T. Glasmacher, Prog. Part. Nucl. Phys **60**, 161 (2008).
[36] S. Szilner, C. A. Ur, L. Corradi, N. Mărginean, G. Pollarolo, A. M. Stefanini, S. Beghini, B. R. Behera, E. Fioretto, A. Gadea, et al., Phys. Rev. C **76**, 024604 (2007).
[37] A. M. Stefanini, L. Corradi, G. Maron, A. Pisent, M. Trotta, A. M. Vinodkumar, S. Beghini, G. Montagnoli, F. Scarlassara, G. F. Segato, et al., Nucl. Phys. **A701**, 217c (2002).
[38] A. Gadea, the EUROBALL Collaboration, and the PRISMA-2 Collaboration, Eur. Phys. J. A **20**, 193 (2004).
[39] A. Poletti, G. Dracoulis, A. Byrne, A. Stuchbery, B. Fabricius, T. Kibèdi, and P. Davidson, Nuclear Physics A **580**, 43 (1994).
[40] Z. M. Wang, Ph.D. thesis, University of the West of Scotland (2010).
[41] C. Chiara and F. Kondev, Nuclear Data Sheets **111**, 141 (2010).
[42] K. Steiger, S. Nishimura, Z. Li, R. Gernhäuser, Y. Utsuno, R. Chen, T. Faestermann, C. Hinke, R. Krücken, M. Kurata-Nishimura, et al., The European Physical Journal A **51**, 1 (2015).
[43] S. R. Stroberg, A. Gade, J. A. Tostevin, V. M. Bader, T. Baugher, D. Bazin, J. S. Berryman, B. A. Brown, C. M. Campbell, K. W. Kemper, et al., Phys. Rev. C **91**, 041302 (2015).
[44] S. Szilner, L. Corradi, F. Haas, D. Lebhertz, G. Pollarolo, C. A. Ur, L. Angus, S. Beghini, M. Bouhelal, R. Chapman, et al., Phys. Rev. C **84**, 014325 (2011).
[45] S. Szilner, private communication.
[46] E. Caurier and F. Nowacki, Acta Phys. Pol. B **30**, 705 (1999).
[47] F. Nowacki and A. Poves, Phys. Rev. C **79**, 014310 (2009).
[48] I. Talmi, Rev. Mod. Phys. **34**, 704 (1962).
[49] J. Cameron, J. Chen, B. Singh, and N. Nica, Nuclear Data Sheets **113**, 365 (2012).
[50] S. Sen, S. Darden, W. Yoh, and E. Berners, Nuclear Physics A **250**, 45 (1975).
[51] C. Nesaraja and E. McCutchan, Nuclear Data Sheets **133**, 1 (2016).
[52] B. Singh and J. A. Cameron, Nuclear Data Sheets **107**, 225 (2006).
[53] B. Bastin, S. Grevy, D. Sohler, O. Sorlin, Z. Dombradi, N. L. Achouri, J. C. Angelique, F. Azaiez, D. Baiborodin, R. Borcea, et al., Phys. Rev. Lett. **99**, 022503 (2007).
[54] A. Hodsdon, R. Chapman, X. Liang, F. Haas, J. Ollier, E. Caurier, F. Nowacki, M. D. Salsac, F. Azaiez, S. Beghini, et al., Phys. Rev. C **75**, 034313 (2007).
[55] J. A. Cameron and B. Singh, Nuclear Data Sheets **109**, 1 (2008).
[56] M. S. Basunia, Nuclear Data Sheets **114**, 1189 (2013).
[57] M. S. Basunia, Nuclear Data Sheets **113**, 909 (2012).
[58] M. S. Basunia, Nuclear Data Sheets **111**, 2331 (2010).
[59] C. Ouellet and B. Singh, Nuclear Data Sheets **114**, 209 (2013).
[60] C. Ouellet and B. Singh, Nuclear Data Sheets **112**, 2199 (2011).
[61] J. Chen and B. Singh, Nuclear Data Sheets **112**, 1393 (2011).
[62] N. Nica and B. Singh, Nuclear Data Sheets **113**, 1563 (2012).
[63] J. Chen, J. Cameron, and B. Singh, Nuclear Data Sheets **112**, 2715 (2011).
[64] N. Nica, J. Cameron, and B. Singh, Nuclear Data Sheets **113**, 1 (2012).
[65] J. A. Cameron and B. Singh, Nuclear Data Sheets **102**, 293 (2004).
[66] J. A. Cameron and B. Singh, Nuclear Data Sheets **94**, 429 (2001).
[67] B. Singh and J. A. Cameron, Nuclear Data Sheets **92**, 1 (2001).
[68] J. A. Cameron and B. Singh, Nuclear Data Sheets **92**, 783 (2001).
[69] J. Chen, B. Singh, and J. A. Cameron, Nuclear Data Sheets **112**, 2357 (2011).
[70] T. Burrows, Nuclear Data Sheets **65**, 1 (1992).
[71] M. Lewis, Nuclear Data Sheets **4**, 237 (1970).
[72] D. Alburger, Nuclear Data Sheets **49**, 237 (1986).